

RM E53B27

~~CONFIDENTIAL~~
~~SECURITY INFORMATION~~

JUN 9 1953



RESEARCH MEMORANDUM

AN INVESTIGATION OF HIGH-FREQUENCY COMBUSTION
OSCILLATIONS IN LIQUID-PROPELLANT
ROCKET ENGINES

By Adelbert O. Tischler, Rudolph V. Massa
and Raymond L. Mantler

Lewis Flight Propulsion Laboratory
Cleveland, Ohio

~~CLASSIFICATION CHANGES~~

To Confidential

By authority of W. L. Roney Date 12/1/53
NACA rel. form # 1625 12/10/53

This material contains information affecting the National Defense of the United States within the meaning of the espionage laws, Title 18, U.S.C., Secs. 793 and 794, the transmission or revelation of which in any manner to an unauthorized person is prohibited by law.

CLASSIFICATION CANCELLED

Authority docs R-93837 Date 7/20/83

See PS/11/8
By W. L. Roney

NATIONAL ADVISORY COMMITTEE FOR AERONAUTICS

WASHINGTON
June 28, 1953

NACA RM E53B27

~~CONFIDENTIAL~~
~~SECURITY INFORMATION~~

LANGLEY AERONAUTICAL RESEARCH CENTER
Langley Field, VA



3 1176 01435 6860

CONFIDENTIAL
SECURITY INFORMATION

NACA RM E53B27

NATIONAL ADVISORY COMMITTEE FOR AERONAUTICS

RESEARCH MEMORANDUMAN INVESTIGATION OF HIGH-FREQUENCY COMBUSTION OSCILLATIONS
IN LIQUID-PROPELLANT ROCKET ENGINESBy Adelbert O. Fischler, Rudolph V. Massa, and
Raymond L. Mantler

SUMMARY

An experimental investigation of high-frequency combustion oscillations (screaming) was conducted with a 100-pound-thrust acid-hydrocarbon rocket engine and a 500-pound-thrust oxygen-fuel rocket engine.

The oscillation frequencies could be correlated as a linear function of the parameter C^*/L , where C^* is the experimentally measured characteristic velocity and L is the combustion-chamber length. The tendency of the engines to scream increased as chamber length was increased.

With engine configurations that normally had a low efficiency, screaming resulted in increased performance; at the same time, a five-to tenfold increase in heat-transfer rate occurred. It was possible, however, to achieve good performance without screaming.

INTRODUCTION

A rocket engine with its combustion chamber, feed lines, propellant valves, pumps, and tanks comprises a large number of potential oscillating systems. The oscillating system may be simply a vibrating mechanical part such as an injector face or a valve, or it may be a more complex hydrodynamic or aerodynamic system involving the flow of propellants through the propellant feed lines or the flow of combustion gases through the chamber and nozzle. Any one of these potential oscillating systems may be driven by the energy available in the rocket combustion process if that energy release is properly pulsed and phased so that a feedback between oscillating system and the energy release occurs (refs. 1 to 4).

One form of combustion-driven oscillations in rocket engines has been identified as a hydrodynamic coupling between combustion-chamber pressure and feed line flow (refs. 5 and 6). This pulsing operation, called chugging, is characterized by frequencies of the order of

CONFIDENTIAL
SECURITY INFORMATION

20 to 200 cycles per second and chamber pressure amplitudes which can stress and fatigue the chamber and which sometimes cause chamber or injector distortion or rupture. Chugging generally results in a loss of specific impulse.

Another type of combustion-driven oscillations, with frequencies from 1000 to 10,000 cycles per second, is characterized by an audible wailing exhaust sound, a bluish, almost invisible exhaust jet in which the shock positions oscillate to make the shock pattern appear fuzzy to the eye, and increased heat transfer to the chamber surfaces. These oscillations, commonly called screaming, often cause chamber, injector, or nozzle burnout failures. Screaming has been observed to increase the specific impulse.

The high-frequency oscillations have been attributed to a combustion-reinforced pressure wave passing through the chamber and reflecting from the chamber surfaces to trigger the succeeding combustion surge. The frequency would therefore be governed by the velocity of wave propagation and the geometry of the chamber. Although the equations for pure acoustical modes cannot be applied rigorously to systems where considerable energy is released periodically in a flowing stream of changing temperature and velocity profile, the oscillation frequencies may be expected to correspond very roughly to one or several simple acoustical modes of the chamber. In cylindrical chambers the prevalent mode would probably be the longitudinal mode corresponding to the closed-closed-end organ pipe frequency (refs. 7 and 8).

A simplified analysis, based on the concept of acoustical resonance, is developed in this report to correlate screaming frequencies with chamber geometry in terms of experimentally measurable quantities. The derived parameter is substantially independent of propellant combination or operating conditions.

The experimental research reported in this paper was undertaken to check the derived relation between the screaming frequency and the rocket combustion-chamber length for two different cylindrical combustion chambers, and to compare the performance and heat-transfer rates of screaming operation with those of nonscreaming or normal operation. Frequency data were obtained with an uncooled 100-pound-thrust acid-hydrocarbon rocket engine and with a water-cooled 500-pound-thrust oxygen-fuel rocket engine. Performance and heat-transfer measurements were obtained for the oxygen-fuel engine with ammonia, JP-3, and alcohol as fuels.

ANALYSIS OF SCREAMING FREQUENCY ON BASIS OF ACOUSTICAL OSCILLATION MODE

If high-frequency oscillations are due to a combustion-driven pressure wave passing through the chamber and reflecting from the chamber surfaces, the frequency of the rocket scream should depend on the

distance of wave travel and the velocity of wave propagation during the completion of an oscillation cycle. For cylindrical combustion chambers the geometry of the chamber can be approximated by a simple tube, closed at the injector end and partly closed at the nozzle end. However, the existence of a choked condition at the throat of a rocket nozzle under operating conditions prohibits the reflection of a compression wave as an expansion wave. Consequently, it may be expected that the rocket chamber is approximated acoustically by a cylinder closed at both ends. For a closed-closed-end cylinder, the frequency f of the longitudinal or axial mode of acoustical oscillation is given by the equation

$$f = \frac{na}{2L}$$

where a is the velocity of wave propagation, L is the cylinder length, and n is a harmonic factor having values 1, 2, 3, 4, to account for multiple standing waves in the chamber.

There is no simple way of estimating the velocity of wave propagation in the chamber from the rocket variables usually measured experimentally. A relation between the characteristic velocity and the velocity of sound at the entrance to the nozzle may be applied

$$C^* = \frac{p_c A_t g}{W} = \frac{a}{\gamma \sqrt{\left(\frac{2}{\gamma+1}\right)^{\frac{\gamma+1}{\gamma-1}}}}$$

where

- C^* characteristic velocity
- p_c chamber pressure
- A_t nozzle throat area
- W total propellant flow
- a acoustic velocity at nozzle entrance
- γ ratio of specific heats

For γ values of interest for rocket exhausts, namely from 1.20 to 1.25, the values of the function of γ vary from 0.7104 to 0.7356. Thus, this function can be assigned a value of 0.72 with an error of less than 2 percent.

5785

CK-1 back

Substituting in the original equation for frequency gives

$$f = \frac{0.72}{2} \frac{n C^*}{L} = \frac{0.36}{L} \frac{n C^*}{L}$$

Similar relations can be derived readily for other acoustical modes of the combustion chamber.

Application of the derived equation to rocket screaming must be recognized as an approximation: first, the acoustical equation does not apply strictly for the case of energy addition within the cycle; second, because of flow through the chamber, the velocity of wave propagation is different in the upstream and downstream directions (this effect on frequency is small for conventional rocket chambers); and third, the velocity of wave propagation in the chamber is not constant at the velocity of sound for the nozzle entrance. For chambers in which the precombustion or low-temperature (low sound velocity) zone is long relative to the chamber length, the average sound velocity may be considerably lower than is indicated by the equations. Conversely, for disturbances of large amplitudes, that is, shock waves, the velocity of wave propagation will exceed the calculated velocity of sound.

In spite of these approximations, the frequency thus derived may be useful in correlating screaming frequencies for various engines because it is substantially independent of propellant type or operating conditions.

APPARATUS AND PROCEDURE

Two rocket setups were used in making these tests. One of these was a 100-pound-thrust acid-hydrocarbon rocket engine (fig. 1) and the other a 500-pound-thrust liquid-oxygen rocket in which three fuels, ammonia, JP-3, and alcohol were used (fig. 2).

100-Pound-Thrust Acid-Hydrocarbon Engine

Chambers and nozzles. - The chambers for the 100-pound-thrust engine were stainless-steel tubes of 2-inch internal diameter used without cooling. Chamber lengths measured from the injector face to the nozzle throat were 8.4, 16.4, 24.4, 32.4, and 40.4 inches (fig. 3(a)). The length-to-diameter ratios varied from 4 to 20 and the characteristic lengths (chamber volume divided by nozzle throat area) from 103 to 516 inches.

The nozzles were convergent nozzles made of aluminum alloy with a 60° convergence half-angle and with a throat diameter of 0.557 inch.

Injector. - A four-acid-on-one-fuel impinging-type injector was used (fig. 3(b)).

Propellants. - Technical grade nitric acid (97 percent HNO_3 , specific gravity, 1.49 - 1.50) was used as oxidant. Commercial n-heptane modified by addition of 12 percent by weight of turpentine was used as a fuel. The turpentine was added to increase the tendency of the rocket to scream.

Instrumentation. - Propellant flows were calculated from the injector pressure drops. The flow rates were calibrated against pressure drop in both the oxidant and the fuel lines with water.

Thrust was measured with a calibrated strain gage. The strain gage output was recorded on a self-balancing potentiometer.

The combustion chamber and injection head pressures were measured with Bourdon-tube pressure recorders.

The combustion oscillation frequencies of the acid-hydrocarbon rocket were determined by three methods. One of these was by use of a piezoelectric crystal pressure pickup. Such a pickup is sensitive to rate of change of pressure rather than to pressure. Therefore the pickup is excellent for frequency determination but of limited value in measuring pressures. The output of the pickup was connected to an oscilloscope and the oscilloscope trace recording by a moving-film camera. Timing marks were printed on the film each 1/120 second. Samples of typical records obtained with the pressure pickup are shown in figure 4(a).

A second method of measuring the screaming oscillation frequency was by use of a moving-film camera set up to photograph the image of the exhaust pattern. The oscillations of the shock patterns in the exhaust jet permit frequency determination. Timing marks of 1/60 second were printed on the record. Sample records are shown in figure 4(b).

The third method of determining screaming frequencies was by use of a microphone and magnetic tape recorder. The microphone was located 20 feet from the rocket engine. Its output was recorded on the tape, which was later played into a panoramic sound analyzer. The sound panoram was photographed and the predominant frequencies read off the photographic record. Typical sound panorams are shown in figure 4(c).

The most complete frequency measurements were undoubtedly obtained by use of the microphone, tape recorder, and panoramic analyzer. This technique, however, is of least accuracy in the frequency measurements because of the necessity for repeatedly calibrating the panoramic

analyzer scale with an audio-oscillator and because of the limited accuracy of reading the spectrum obtained with the instrument. The data obtained with the panoramic analyzer show an absence of frequencies above 4000 cycles per second. This absence of recorded high frequencies is believed caused, in part at least, by the reduced response of the amplification equipment in the microphone, tape recorders, and panoramic analyzer circuitry. A large amount of low-amplitude noise appeared on the sound panoramas. This noise was also present in nonscreaming runs. These frequencies were eliminated from the screaming data plotted by arbitrarily discarding all frequencies less than one-third of the maximum amplitude on the logarithmic decibel scale. Agreement within experimental uncertainty was found in measurement of the fundamental oscillation frequency by the three methods.

Procedure. - The rocket was operated at various chamber pressures from 150 to 350 pounds per square inch and oxidant-fuel ratios from 2.0 to 6.5 for each of the combustion-chamber lengths. A slug of furfuryl alcohol in the fuel line was used for hypergolic (spontaneous ignition) starts. Runs were of about 5 seconds duration.

500-Pound-Thrust Oxygen-Fuel Engine

Chambers and nozzles. - The combustion chambers for the 500-pound-thrust engine were annular water-jacketed tubes of 4-inch internal diameter. Tube lengths measured to the nozzle throat were 21, 27, 35, and 41 inches. The nozzle was a water-cooled nozzle of 30° convergent and 10° divergent half-angles with a 1.235-inch-diameter throat (fig. 5(a)). The length-to-diameter ratios varied from 2.0 to 9.5 and the characteristic lengths from 105 to 437 inches.

Injectors. - Three injectors were used. Most screaming runs were made with a showerhead-type injector with six concentric rings of jets; three rings, each with 12 fuel holes, surrounding three rings, each with 8 oxygen holes (fig. 5(b)).

An impinging-jet-type injector used had 24 fuel jets surrounding 12 oxygen jets. The holes were arranged so that 12 of the fuel jets impinged directly on the oxygen jets (fig. 5(c)).

The third type of injector used was called a spray injector. It had 24 fuel jets impinging into a spray of oxygen which emerged from a swirl chamber (fig. 5(d)).

Propellants. - Commercial liquid oxygen was used as the oxidizer. Three fuels were used: (1) anhydrous commercial liquid ammonia, (2) JP-3, and (3) alcohol, which assayed 95 percent ethyl alcohol and 5 percent methyl alcohol.

Instrumentation. - The propellant flows were measured continuously by strain gages supporting counterbalanced tanks.

The thrust of the rocket engine was measured by strain gages connected to a parallelogram-frame thrust stand. The outputs of the weighing and thrust strain gages were recorded on self-balancing potentiometers.

Combustion-chamber pressure was measured on a Bourdon-tube-type circular chart recorder.

The coolant temperatures into and out of the chamber were measured by copper-constantan thermocouples. The thermocouple outputs were recorded on self-balancing potentiometers.

The coolant water flow rate during the run was determined by measurement of the pressure drop across the coolant jacket. Calibration prior to running gave the relation between coolant flows and pressure drop.

The combustion-oscillation frequencies were determined by recording the output of a microphone on magnetic tape. The microphone was located in the rocket cell. The tape records were played back into a panoramic sound analyzer to separate the frequencies present in the sound spectra. Only the predominant frequencies with amplitudes greater than one-third the maximum amplitude were recorded.

Procedure. - Ignition of the engine was accomplished by use of a spark igniter inserted through the nozzle. The engine was started with throttled propellant flows and brought up to full thrust in about 2 seconds.

Screaming was initiated by adjustment of the oxidant-fuel ratio and chamber pressure. With the showerhead-type injector, screaming generally occurred from 2 to 5 seconds after full thrust was reached. No screaming runs were obtained with the spray-type injector.

The effects of the combustion-chamber length on the screaming frequency were investigated with both engines. In addition an effort to correlate screaming data obtained at several other rocket laboratories was made.

Performance and heat-transfer measurements under normal and screaming operation were made with the oxygen engine with ammonia, JP-3, and alcohol as fuels.

RESULTS AND DISCUSSION

Effect of Combustion-Chamber Length on

Frequency of Screaming

100-Pound-thrust acid-hydrocarbon rocket engine. - The observed screaming frequencies for the 100-pound-thrust acid-hydrocarbon rocket engine are plotted in figure 6(a) against the ratio of the characteristic velocity to the combustion-chamber length (C^*/L); the equation $f = 0.36n C^*/L$ is also plotted. Use of this parameter permits correlation of frequency data over a range of propellant performance values as well as for different propellant combinations (see ANALYSIS section). The several methods used for measuring screaming frequencies with the acid-hydrocarbon rocket show substantial agreement for the low or fundamental screaming frequencies. For the pressure pickup records, observation of frequencies higher than the third harmonic was difficult because of the problem of distinguishing these higher frequencies on the film trace. The moving-film records of the oscillations in the shock patterns of the exhaust jet indicated a predominance of the fundamental frequency in all cases. Higher frequencies than this were not discernible on the records.

The plotted data show substantial agreement with the theoretical lines derived in the ANALYSIS section for the longitudinal acoustical mode. The agreement between analysis and experimental fundamental frequency confirms the assumption that the chamber behaves essentially like a closed-closed-end organ pipe, since the fundamental for an organ pipe with one open end would be half the lowest frequencies observed here. However, to assume that the harmonics which appear in the panoramic records are due to multiple standing waves in the chamber may be erroneous. Typical pressure traces obtained in screaming rockets indicate the propagation of a steep-fronted wave. Such a trace can be resolved by Fourier-series analysis to a series of sinusoidal waves of frequencies harmonic to the fundamental frequency; the panoramic analyzer performs this resolution. Because of the improbability that the multiple frequencies indicated by the data coexist as separate waves in the chamber, it seems likely that these apparent harmonics are actually the Fourier-series components of the nonsinusoidal pressure disturbance.

The screaming frequencies for the long chambers (low C^*/L values) lie above the theoretical line. In order to obtain frequencies above the theoretical, it is necessary either that the wave velocity be greater or the chamber length less than the values used. The uncertainty of the chamber length, particularly for the long acid-hydrocarbon engines, for which the total correction for the nozzle length is about 1 percent, appears negligibly small. Therefore, it is evident that the wave propagation velocity is greater than the calculated acoustical velocity at the nozzle entrance. This may indicate high-intensity or shock-type wave propagation in the chamber. That shock-type wave propagation occurs

in screaming rockets has already been shown by Berman and Cheney (ref. 11), who estimated the strength of the shock, that is, the ratio of static pressure behind the shock to static pressure in front of the shock, as 1.5 in their 1500-pound-thrust oxygen-alcohol engine.

For the short chambers, on the other hand, the screaming frequencies lie below the acoustical curve. This is probably due to the low mean acoustical velocity in the short chambers, which have proportionally longer low-temperature zones than the long chambers.

500-Pound-thrust oxygen-fuel rocket. - The relation between the frequency of screaming and the parameter C^*/L for the 500-pound liquid oxygen-ammonia rocket engine is plotted in figure 6(b). Again the experimentally measured frequencies show agreement with the longitudinal or organ-pipe acoustical mode. The panorams show the presence of all harmonic frequencies up to the reduced analyzer response.

Survey of data from other laboratories. - Screaming data obtained from other laboratories are plotted in figure 6(c). Wherever the geometry and sufficient information to estimate the experimental performance were given, the frequency data were plotted against the parameter C^*/L . The chamber lengths were taken from the injector to the throat of the nozzle. In most of these instances the combustion chambers were relatively short with length-to-diameter ratios and characteristic lengths considerably less than those for the chambers used for figures 6(a) and 6(b). This may account for the fact that the experimentally observed frequencies lie on a line about 80 percent of the theoretical frequencies. Data for rocket engines beyond 5000 pounds thrust were not available for this plot. A recent paper by Levine and Lawhead (ref. 9), presumably on high-thrust engines, discusses frequencies which do not correlate with the axial dimension of the rocket but rather with the diameter. It seems likely that in large-scale engines, where the cylinder length-to-diameter ratio becomes proportionally less than for low-thrust chambers, radial and transverse acoustical oscillations will be more apparent.

The correlation between experimentally measured screaming frequency and the frequency calculated on the basis of acoustical theory agrees with observations reported in reference 10. Reference 11 also shows experimental screaming frequencies for a 1200-pound-thrust liquid oxygen-alcohol rocket engine. By use of the correlation parameter, the C^* of the engine can be calculated. The value obtained for C^* is 5160 feet per second, which is a reasonable value.

These results indicate that screaming is due to a combustion-driven pressure wave reflecting in the chamber and that, for low-thrust chambers at least, a prevalent mode of oscillation of the chamber is the axial or longitudinal mode.

Effect of screaming on performance. - Specific impulse data for the 500-pound-thrust oxygen rocket with ammonia as fuel are shown in figure 7 for the three different injectors in a 32-inch chamber. With the showerhead-type injector, which had poor performance under normal operations, a large increase in performance, from about 70 percent to 90 percent of theoretical for equilibrium expansion, was experienced when screaming occurred.

With the impinging-jet-type injector, one normal run indicated higher specific impulse than the screaming runs. The differences in performance, however, were of the order of the experimental uncertainty. Performance in both cases was high.

With the spray injector, no screaming runs were obtained. The specific impulse with this injector was equivalent to the specific impulse with the showerhead-type injector under screaming operation. These results indicate that high propellant performance in a rocket engine can be achieved without screaming operation.

Some performance data were obtained with the showerhead-type injector with JP-3 as the fuel. These are shown in the following table. The injector was not modified for use of the different fuel; consequently, a mismatch of oxidant and fuel injector pressure drops was inherent in the setup.

Oxidant-fuel ratio	Theoretical specific impulse, lb-sec/lb	Normal specific impulse, lb-sec/lb	Screaming specific impulse, lb-sec/lb
2.13	263	191	
2.30	262		245

As with the ammonia fuel, the showerhead-type injector gave poor performance under normal operation and high performance under screaming operation. The data show that screaming can increase the performance of a low-efficiency engine.

Effect of Screaming on Heat Transfer

The over-all heat-transfer rates for the 500-pound-thrust rocket are shown for liquid oxygen-ammonia with the showerhead-type injector in figure 8. Over-all heat-transfer rates for the showerhead-type injector with JP-3 and alcohol fuels with liquid oxygen are:

Fuel	Oxidant-fuel ratio	Heat-transfer rate, Btu/sec/sq in.	
		Normal	Screaming
JP-3	2.25	0.65	2.85
	2.29		
	2.84	.63	
Alcohol	1.42	0.49	2.75 2.50
	1.44	.55	
	1.45	.54	
	1.66		
	1.92		

With the showerhead-type injector, all screaming test runs gave greatly increased heat-transfer rates. For the ammonia the increase was about tenfold, and for JP-3 and alcohol, about fivefold. At least a part of these differences is attributable to the fact that higher specific impulses were obtained with screaming than with normal operation (see previous section).

Calculations of the convective and radiant heat transfer (see appendix) under the two conditions of operation indicate that the increase of heat transfer under screaming conditions was somewhat greater than was calculated on the basis of the increased performance. This difference suggests the possibility that some phenomenon, either aerodynamic or radiation heat transfer, augments the heat-transfer mechanisms during screaming operation.

The heat-transfer rates for the nonscreaming spray injector with ammonia fuel are also shown in figure 8. These were about 30 percent less than those for the showerhead-type injector under screaming conditions. These rates are for approximately equivalent specific impulses.

Effect of Chamber Length on Tendency for Screaming

Several hundred runs were made with the 100-pound-thrust acid-hydrocarbon rocket engine. The percentage of screaming runs for each different combustion-chamber length was calculated and the results are shown in figure 9. Each data point represents from 24 to 92 runs. The plot shows an increasing tendency for screaming operation as the combustion-chamber length is increased.

Observations

Screaming operation was generally preceded by a period of rough burning. Pressure pickup records indicated a series of minor explosions just prior to screaming. With alcohol fuel these initiating explosions

were sufficiently violent to disrupt the thrust strain gage; consequently, no specific impulse data were obtained with alcohol fuel. This experience differs from that of reference 11, in which a smooth transition to high-frequency combustion oscillation was indicated. Once started, screaming was stable and could not be stopped except by shutdown.

In the oxygen-fuel rocket the oscillations were found prone to occur in the oxidant-rich region. With the showerhead-type injector screaming occurred only after the propellant lines had cleared of oxygen warmed before the run and when the colder oxygen from the tank was entering the rocket chamber. When the oxygen temperature was raised about 50° F (by pressurizing the tank and allowing the oxygen temperature to rise), no screaming occurred. With the impinging-jet-type injector the opposite effect was observed: when screaming occurred it began immediately at the start of the run and it occurred most readily if the oxygen temperature was raised. The observations imply that the screaming propensity is linked with atomization and vaporization processes caused by the injector.

The exhaust flames of the rocket engines changed when screaming occurred. The exhaust of the acid-hydrocarbon rocket changed from a faint yellow (candle-like) color to a faint blue. With ammonia fuel the flame of the oxygen rocket became invisible. The exhaust flames with JP-3 and alcohol changed from yellowish to a transparent blue color. The shock pattern in all cases appeared undefined during screaming.

The correlation of the experimental data with the analysis and the fact that screaming occurred in the rather heavily constructed acid-hydrocarbon rocket engine negate the suggestion that the screaming in these engines may be caused by mechanical vibrations of the chamber walls or injector. In addition, an uncooled chamber with 1/2-inch wall thickness was fitted with one of the test injectors on the oxygen stand. Screaming combustion also occurred in this chamber.

SUMMARY OF RESULTS

Screaming data from two rocket engines, one a 100-pound-thrust uncooled acid-hydrocarbon rocket and the other a 500-pound-thrust water-cooled liquid oxygen-fuel rocket, indicate:

1. The screaming frequencies in these cylindrical rocket chambers corresponded roughly to the frequencies of a closed-closed-end organ-pipe resonance and correlated with the parameter C^*/L where C^* is the characteristic velocity and L the combustion-chamber length.

2. Performance with a poor injector-chamber configuration was increased by screaming operation; however, good performance was achieved without screaming with a good injector-chamber configuration.

3. Heat transfer to the rocket chamber surfaces was increased when screaming occurred. For an oxygen-ammonia rocket, the increase was from 0.2 Btu per second per square inch under normal operation to 2 Btu per second per square inch under screaming conditions; this corresponded to an increase in specific impulse from 70 percent of theoretical under normal operation to 90 percent of theoretical under screaming operation. Calculations of the convective and radiant heat transfer under the two conditions of operation indicate that the increase of heat-transfer under screaming conditions was somewhat greater than was expected from the increased performance.

4. The acid-hydrocarbon rocket indicated an increased tendency to scream as the rocket chamber length was increased.

5. The oxygen temperature affected the tendency of the liquid oxygen-ammonia rocket to scream. With a showerhead-type injector, raising the oxygen temperature before injection into the engine reduced the tendency to scream. With an impinging-jet-type injector, raising the oxygen temperature increased the tendency to scream.

6. Screaming occurred in thick-walled cylinders as well as in thin-walled cylinders.

Lewis Flight Propulsion Laboratory
National Advisory Committee for Aeronautics
Cleveland, Ohio

APPENDIX - CALCULATION OF HEAT TRANSFER IN OXYGEN-AMMONIA
ROCKET ENGINE

The equations from which the heat transfer for the oxygen-ammonia rocket engine is estimated are set forth by McAdams (ref. 12).

Convective Heat Transfer

The equation for convective heat transfer where the gas-film heat transfer is the controlling heat-transfer step may be written:

$$\frac{q_c}{A} = h_g \Delta T = 0.023 \frac{\kappa}{D} \left(\frac{Dv\rho}{\mu} \right)^{0.8} \left(\frac{\mu c_p}{\kappa} \right)^{0.3} \Delta T$$

where

q_c convective heat transfer to wall, Btu/(sec)(°R)(sq ft)

A area of wall, sq ft

h_g film coefficient, Btu/(sec)(°R)(sq ft)

ΔT temperature difference, °R

κ conductivity of gas, Btu/(sec)(sq ft)(°R/ft)

D chamber diameter, ft

v average local gas velocity, ft/sec

ρ gas density, lb/cu ft

μ absolute gas viscosity, lb/ft-sec

c_p specific heat of gas, Btu/(°R)(lb)

Since the theoretical maximum flame temperature for the oxygen-ammonia combination is approximately 5360° R, which corresponds to a specific impulse of 258 pound-seconds per pound, and since the experimentally measured specific impulse was 95 percent of the theoretical, the maximum flame temperature T_g in the chamber was assumed to be

$$T_g = 5360 \times 0.95^2 = 4830^\circ \text{ R}$$

And the weight flow of propellants W was estimated from thrust F and the specific impulse I_{sp} :

$$W = \frac{F}{I_{sp}} = \frac{500}{245} = 2.04 \text{ lb/sec}$$

The quantity Dv_p can be rewritten $4W/\mu\pi D$; for this chamber $D = 1/3$ foot. For the assumed flame temperature,

$$\kappa = 43.8 \times 10^{-6} \text{ Btu/(sec)(sq ft)(}^\circ\text{R/ft)}$$

$$\mu = 53.8 \times 10^{-6} \text{ lb/ft-sec}$$

$$c_p = 0.88 \text{ Btu/(}^\circ\text{R)(lb)}$$

and

$$\frac{4W}{\mu\pi D} = \frac{Dv_p}{\mu} = 1.45 \times 10^5$$

$$\frac{\mu c_p}{\kappa} = 1.08$$

Therefore

$$h_g = \frac{43.8 \times 10^{-6} \times 0.023}{0.333} (1.45 \times 10^5)^{0.8} (1.08)^{0.3}$$

$$= 0.0418 \text{ Btu/(sec)(}^\circ\text{R)(sq ft)}$$

$$= 2.9 \times 10^{-4} \text{ Btu/(sec)(}^\circ\text{R)(sq in.)}$$

If the inside wall temperature is assumed to be 1060° R

$$\Delta T = 4830 - 1060 = 3770^\circ \text{ R}$$

Then the convective heat-transfer rate in the chamber is

$$\frac{q_c}{A} = h_g \Delta T = 1.09 \text{ Btu/(sec)(sq in.)}$$

The heat transfer in the nozzle q_n is a little more difficult to compute because of the changing cross-section and aerodynamic flow. An approximate expression for heat transfer can be derived by integrating the convective heat-transfer equation:

$$q_n = \Delta T \left(\int_{D_o}^{D_t} h_g dA + \int_{D_t}^{D_e} h_g dA \right)$$

where D_o , D_t , and D_e are the chamber, throat, and exit diameters of the nozzle, respectively, and

$$h_g = 0.023 \frac{\kappa}{D} \left(\frac{4W}{\mu \pi D} \right)^{0.8} \left(\frac{\mu c_p}{\kappa} \right)^{0.3}$$

If the nozzle is assumed to be two truncated cones joined at the nozzle throat, the change in nozzle area can be expressed in terms of the distance x from the chamber end of the nozzle. For the convergent section $dA = -\pi D \sec \alpha dx$ and for the divergent section $dA = \pi D \sec \alpha dx$ where α and β are the convergent and divergent half-angles of the nozzle.

It is desirable to express these area changes as functions of the diameters. Since

$$dx_{\text{conv}} = -\cot \alpha dD$$

$$dx_{\text{div}} = \cot \beta dD$$

it follows that

$$dA_{\text{conv}} = \frac{\pi D dD}{2 \sin \alpha}$$

and

$$dA_{\text{div}} = \frac{\pi D dD}{2 \sin \beta}$$

Now the heat transfer can be expressed

$$q_n = \Delta T \left[\int_{D_o}^{D_t} \frac{0.023}{D} \kappa \left(\frac{4W}{\mu\pi} \right)^{0.8} \left(\frac{1}{D} \right)^{0.8} \left(\frac{\mu c_p}{\kappa} \right)^{0.3} \frac{\pi D dD}{2 \sin \alpha} + \int_{D_t}^{D_e} \frac{0.023 \kappa}{D} \left(\frac{4W}{\mu\pi} \right)^{0.8} \left(\frac{1}{D} \right)^{0.8} \left(\frac{\mu c_p}{\kappa} \right)^{0.3} \frac{\pi D dD}{2 \sin \beta} \right]$$

For purposes of simplification the gas properties are assumed constant. Then the expression can be integrated

$$q_n = 0.023 \frac{\pi \kappa \Delta T}{2 \cdot 0.2} \left(\frac{4W}{\mu\pi} \right)^{0.8} \left(\frac{\mu c_p}{\kappa} \right)^{0.3} \left[- \frac{(D_t)^{0.2} - (D_o)^{0.2}}{\sin \alpha} + \frac{(D_e)^{0.2} - (D_t)^{0.2}}{\sin \beta} \right]$$

which can be rewritten

$$q_n = \frac{0.181 \kappa}{\sin \alpha} \Delta T \left(\frac{4W}{\mu\pi} \right)^{0.8} \left(\frac{\mu c_p}{\kappa} \right)^{0.3} \left[D_o^{0.2} - \left(1 + \frac{\sin \alpha}{\sin \beta} \right) D_t^{0.2} + \frac{\sin \alpha}{\sin \beta} D_e^{0.2} \right]$$

From this equation the heat transfer in the rocket nozzle was estimated. The temperature throughout the nozzle was assumed constant and equal to the flame temperature $\alpha = 30^\circ$; $\beta = 10^\circ$; $D_t = 1.235$ inches; and $D_e = 2.130$ inches.

$$q_n = 0.181 \frac{43.8 \times 10^{-6}}{0.5} (3770) (4.83 \times 10^4)^{0.8} 1.08^{0.3} \left[0.333^{0.2} - 3.88 (0.103)^{0.2} + 2.88 (0.1775)^{0.2} \right]$$

$$q_n = 130 \text{ Btu/sec}$$

Although the temperature of the boundary layer through the nozzle is generally assumed to be equal to the total temperature of the gases rather than the static temperatures, the value calculated on the basis of constant (total) temperature is again probably high.

The over-all convective heat-transfer rate for the chamber and nozzle can be calculated from the previously given results and the respective areas. The area of the chamber was 402 square inches; the area of the nozzle was 45 square inches. The over-all heat-transfer rate is

$$\begin{aligned} \frac{q_o}{A} &= \frac{(q_c/A) A_c + q_n}{A_c + A_n} \\ &= \frac{(1.09)(402) + 130}{402 + 45} \\ &= 1.40 \text{ Btu}/(\text{sec})(\text{sq in.}) \end{aligned}$$

Radiant Heat Transfer

The radiant heat transfer in the rocket chamber is estimated from the equation

$$\frac{q_r}{A} = 0.173 \epsilon'_s \left[\epsilon_g \left(\frac{T_g}{100} \right)^4 - \alpha_g \left(\frac{T_s}{100} \right)^4 \right]$$

q_r heat-transfer rate, Btu/(hr)(sq ft)

ϵ'_s pseudo-emissivity of chamber wall

ϵ_g emissivity of gas

T_g temperature of gas, °R

α_g emissivity of gas at wall temperature

T_s wall temperature

The factor $\alpha_g(T_s/100)^4$ is considered negligible in these calculations because of the low value of T_s .

The radiant heat transfer from the exhaust gases of an oxygen-ammonia flame is due almost entirely to the radiation from the water formed in the combustion reaction. The emissivity can be estimated from the gas temperature and the product of the water pressure and effective beam length.

The gas temperature is, as before, 4830° R. The partial pressure of water p_w is its mole fraction times the chamber pressure.

$$p_w = 0.65 \times 20.4 = 13.2 \text{ atm}$$

The effective beam length L for a cylinder is taken as 0.9 of the diameter. Therefore,

$$p_w L = 13.2 \times 0.3 = 4 \text{ ft-atm}$$

For which

$$\epsilon_w = 0.14 \text{ (see ref. 12)}$$

The pseudo-emissivity of the chamber walls is taken halfway between the estimated wall emissivity and one. The relatively small contribution of radiation to the over-all heat-transfer rate justifies this crude approximation.

$$\epsilon'_s = \frac{0.2 + 1}{2} = 0.6$$

Then

$$\begin{aligned} \frac{q_r}{A} &= 0.173 (0.6) (0.14) \left(\frac{4830}{100} \right)^4 \\ &= 7.9 \times 10^4 \text{ Btu/(hr)(sq ft)} \\ &= 0.15 \text{ Btu/(sec)(sq in.)} \end{aligned}$$

Because of the short beam lengths in the nozzle the radiant heat transfer in the nozzle section is neglected.

Over-All Heat Transfer

The over-all heat-transfer rate is the sum of the estimated convective and radiant heat-transfer rates

$$\begin{aligned} q_f &= q_c + q_r \\ &= 1.40 + 0.15 = 1.55 \text{ Btu/(sec)(sq in.)} \end{aligned}$$

This value should be slanted toward a high heat-transfer rate since the calculations assume the flame temperature to exist throughout the chamber and nozzle.

REFERENCES

1. Rayleigh: The Theory of Sound. Vol. II. Dover Pub., 1945.
2. Blackshear, Perry L., Jr.: Driving Standing Waves by Heat Addition. NACA TN 2772, 1952.
3. Crocco, L.: Aspects of Combustion Stability in Liquid Propellant Rocket Motors. Part I: Fundamental Low Frequency Instability with Monopropellants. Jour. Am. Rocket Soc., vol. 21, no. 6, Nov. 1951, pp. 163-178.
4. Crocco, L.: Aspects of Combustion Stability in Liquid Propellant Rocket Motors. Part II. Low Frequency Instability with Bipropellants. High Frequency Instability. Jour. Am. Rocket Soc., vol. 22, no. 1, Jan.-Feb. 1952, pp. 7-16.
5. Tischler, Adelbert O., and Bellman, Donald R.: Combustion Instability in an Acid-Heptane Rocket with a Pressurized-Gas Propellant Pumping System. NACA TN 2936, 1953.
6. Summerfield, Martin: A Theory of Unstable Combustion in Liquid Propellant Rocket Systems. Jour. Am. Rocket Soc., vol. 21, no. 5, Sept. 1951, pp. 108-114.
7. Berman, Kurt, and Logan, Stanley E.: Combustion Studies with a Rocket Motor Having a Full-Length Observation Window. Jour. Am. Rocket Soc., vol. 22, no. 2, Mar.-Apr. 1952, pp. 78-85.
8. Elias, I., and Gordon, Robert: Longitudinal Vibrations of Gas at Ambient Pressure in a Rocket Thrust Chamber. Jour. Am. Rocket Soc., vol. 22, no. 5, Sept.-Oct. 1952, pp. 263-268.
9. Levine, R. S., and Lawhead, R. W.: A Survey of Combustion Instability in Liquid Propellant Rocket Engines. Paper No. 63-52 presented before Am. Rocket Soc., New York (N. Y.), Dec. 1-6, 1952. (See also Aviation Age, vol. 19, no. 1, Jan. 1953, pp. 50-55.)
10. Ellis, Herbert, Odgers, Irving, Stosick, A. J., Van De Verg, N., and Wick, R. S.: Experimental Investigation of Combustion Instability in Rocket Motors. Paper No. 6, Abs. of papers presented at Fourth Symposium on Combustion, M.I.T., Cambridge (Mass.), Sept. 1-5, 1952, pp. 8-9.
11. Berman, Kurt, and Cheney, Samuel H., Jr.: Combustion Studies in Rocket Motors. Paper No. 65-52 presented before Am. Rocket Soc., New York (N. Y.), Dec. 1-6, 1952. (See also Discussion, Aviation Age, vol. 19, no. 2, Feb. 1953, pp. 46-47.)

12. McAdams, William H.: Heat Transmission. Second ed., McGraw-Hill Book Co., Inc., 1942.

2845

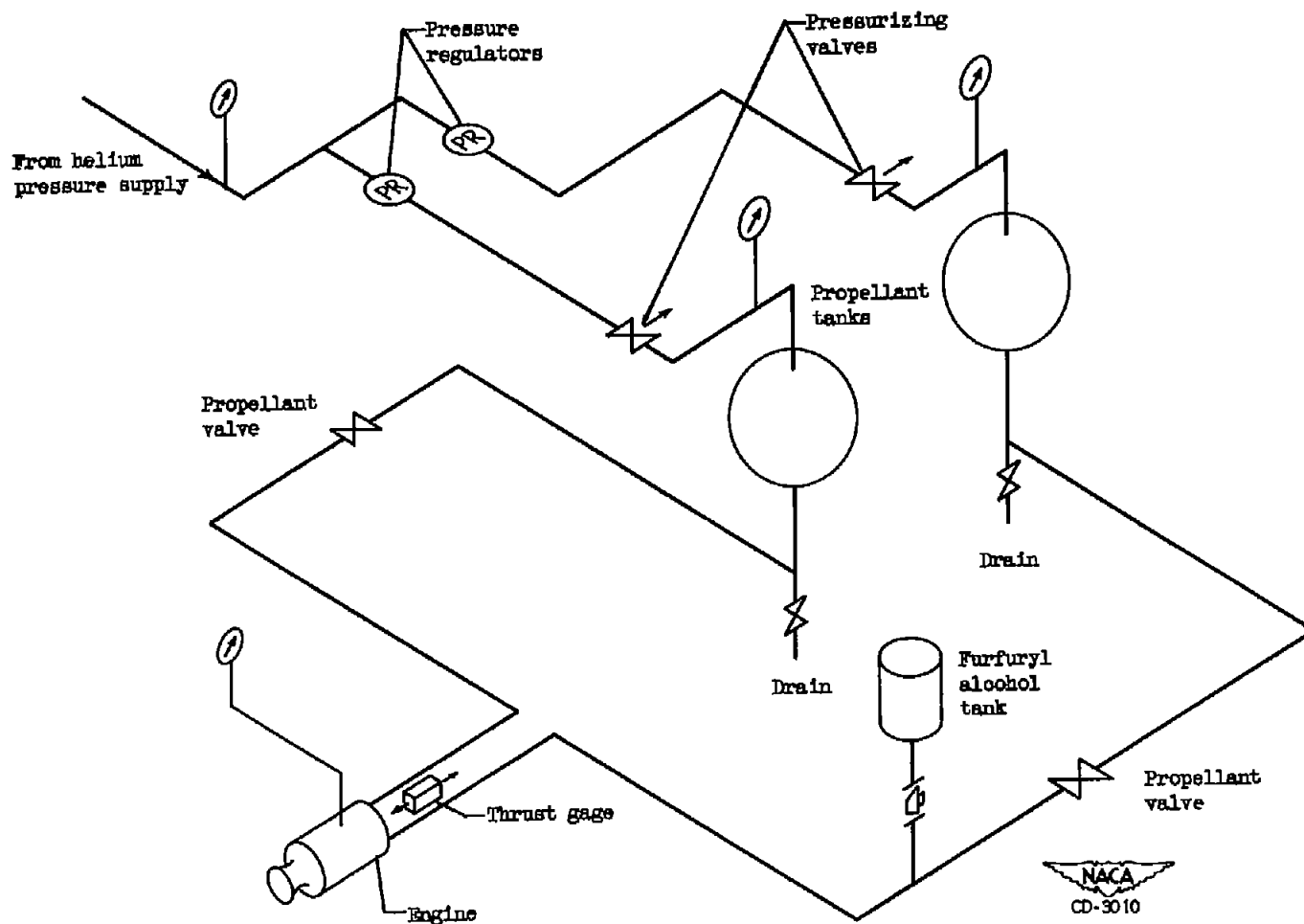


Figure 1. - Schematic layout of 100-pound-thrust acid-hydrocarbon rocket engine.

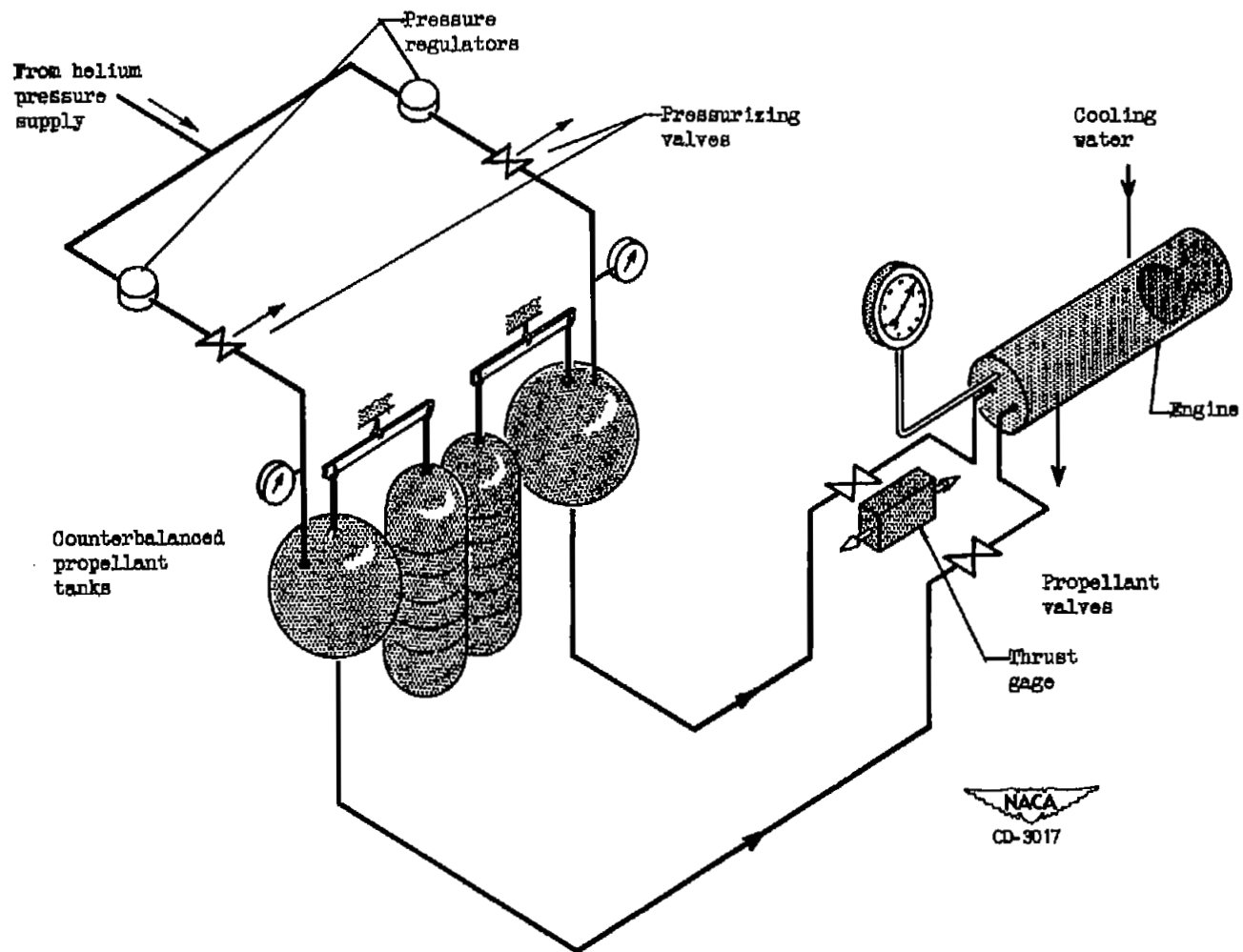


Figure 2. - Schematic layout of 500-pound-thrust oxygen-fuel rocket engine.

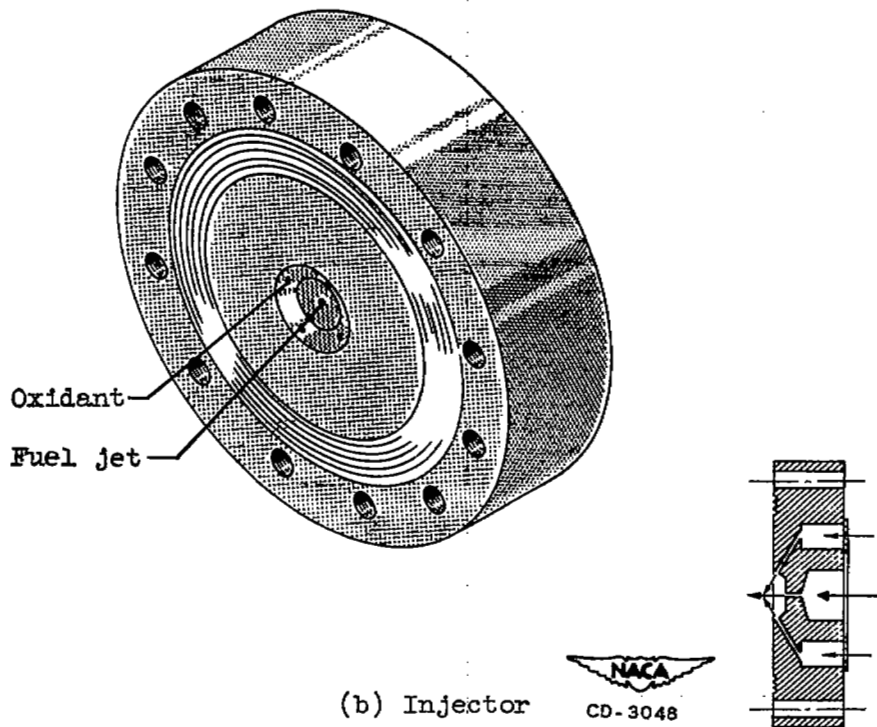
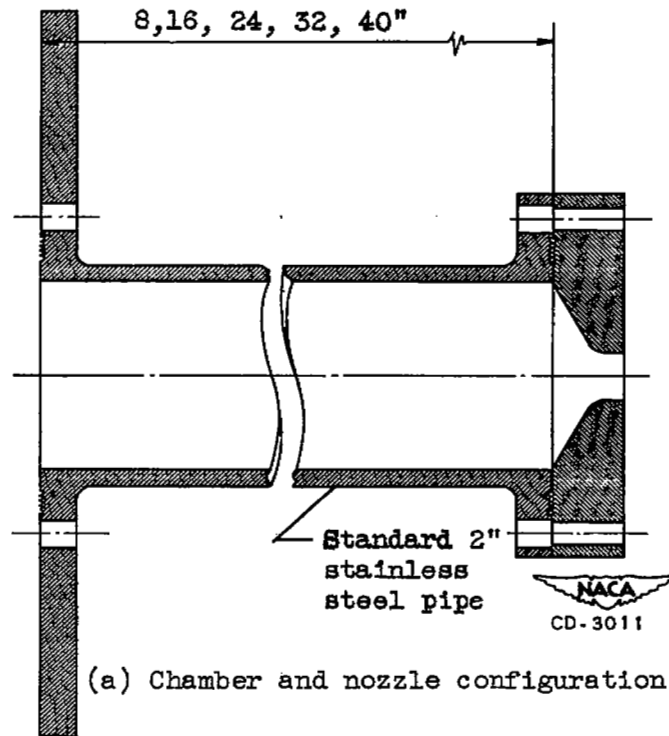


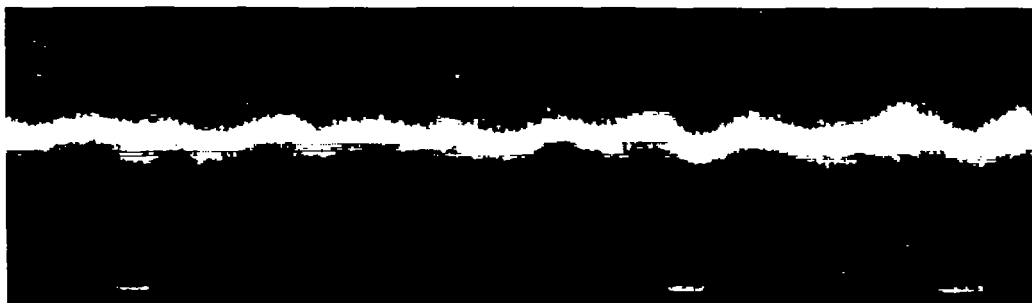
Figure 3. - Diagrams of 100-pound-thrust acid-hydrocarbon rocket engine.

2845



← 1/60 sec →

Normal operation

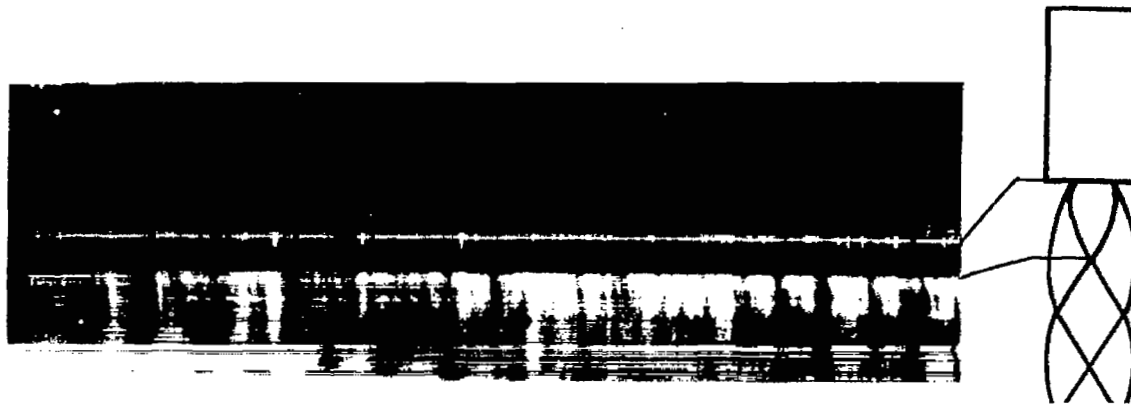


Screaming operation

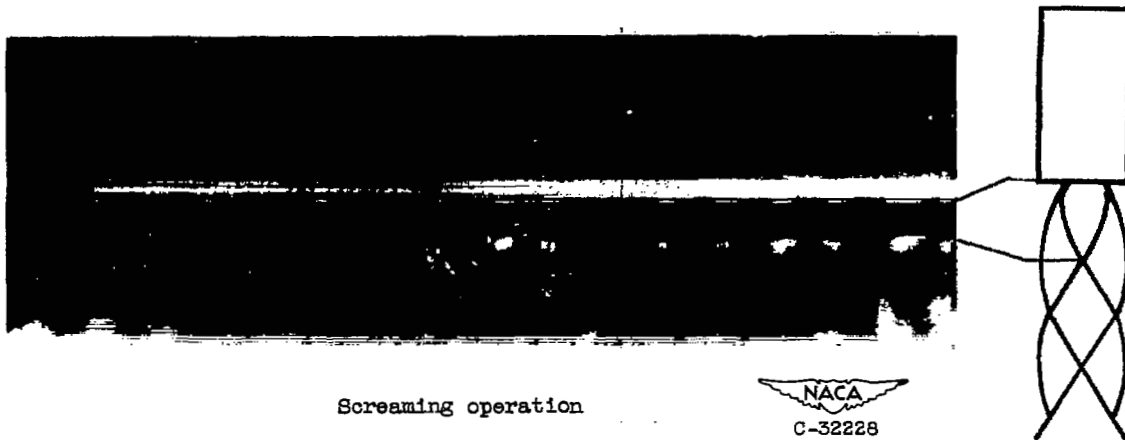
NACA
C-32227

(a) Oscillograph traces obtained with piezoelectric pressure detector.

Figure 4. - Samples of records used to determine screaming frequencies.



Normal operation



Screaming operation

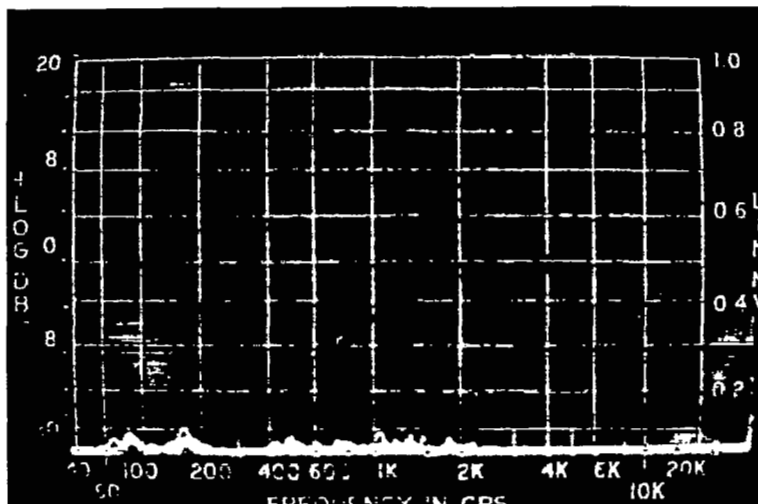
NACA
C-32228

(b) Moving film photographs of exhaust jet.

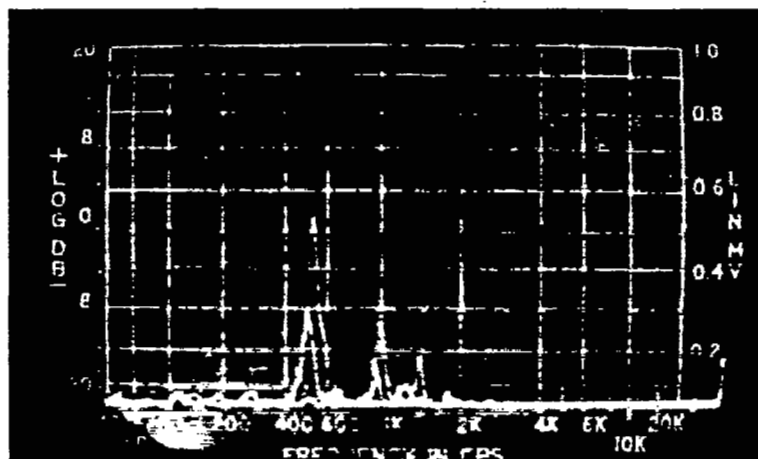
Figure 4. - Continued. Samples of records used to determine screaming frequencies.

2845

CK-4 back



Normal operation

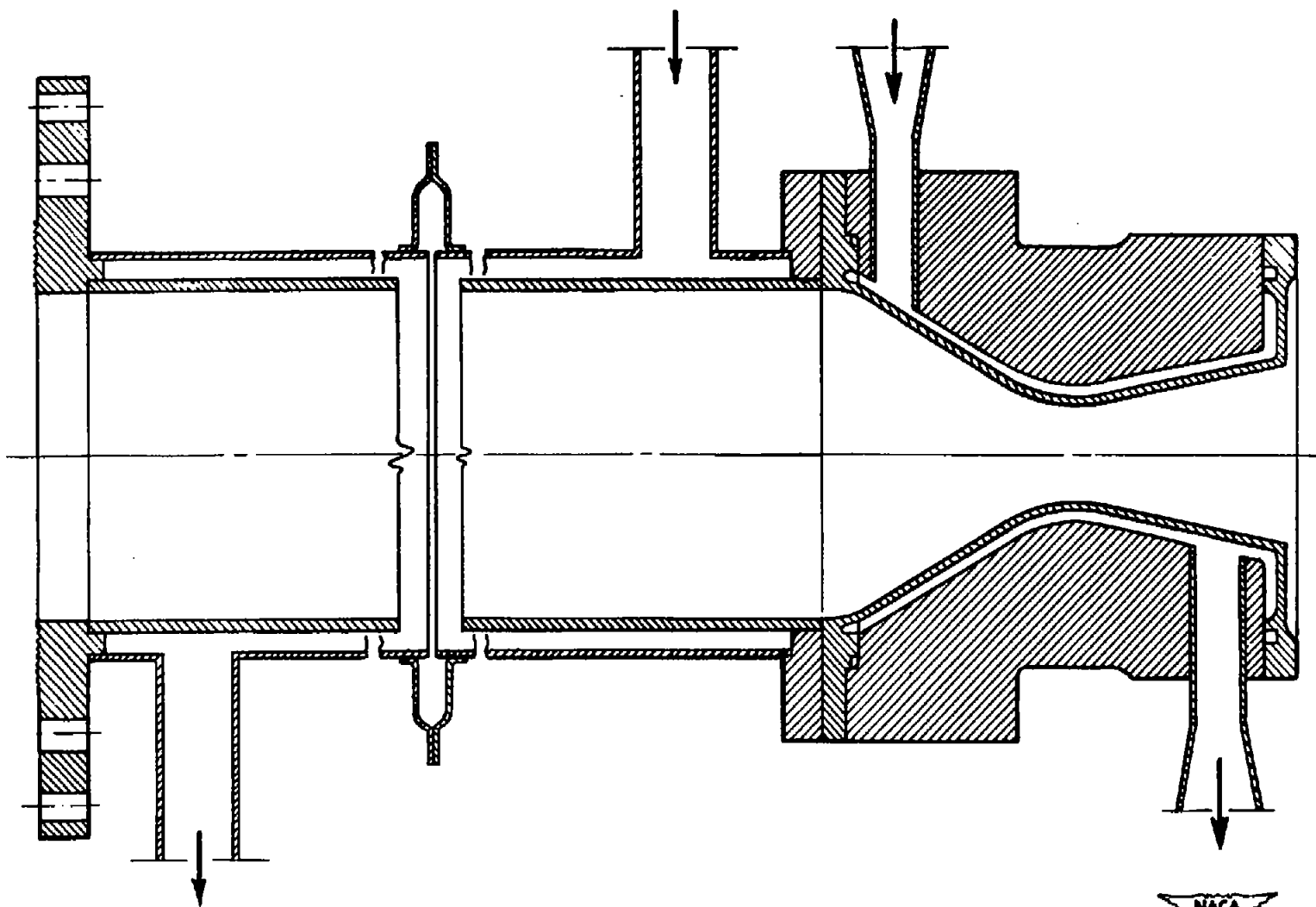


Screaming operation



(c) Panoramic sound records.

Figure 4. - Concluded. Samples of records used to determine screaming frequencies.

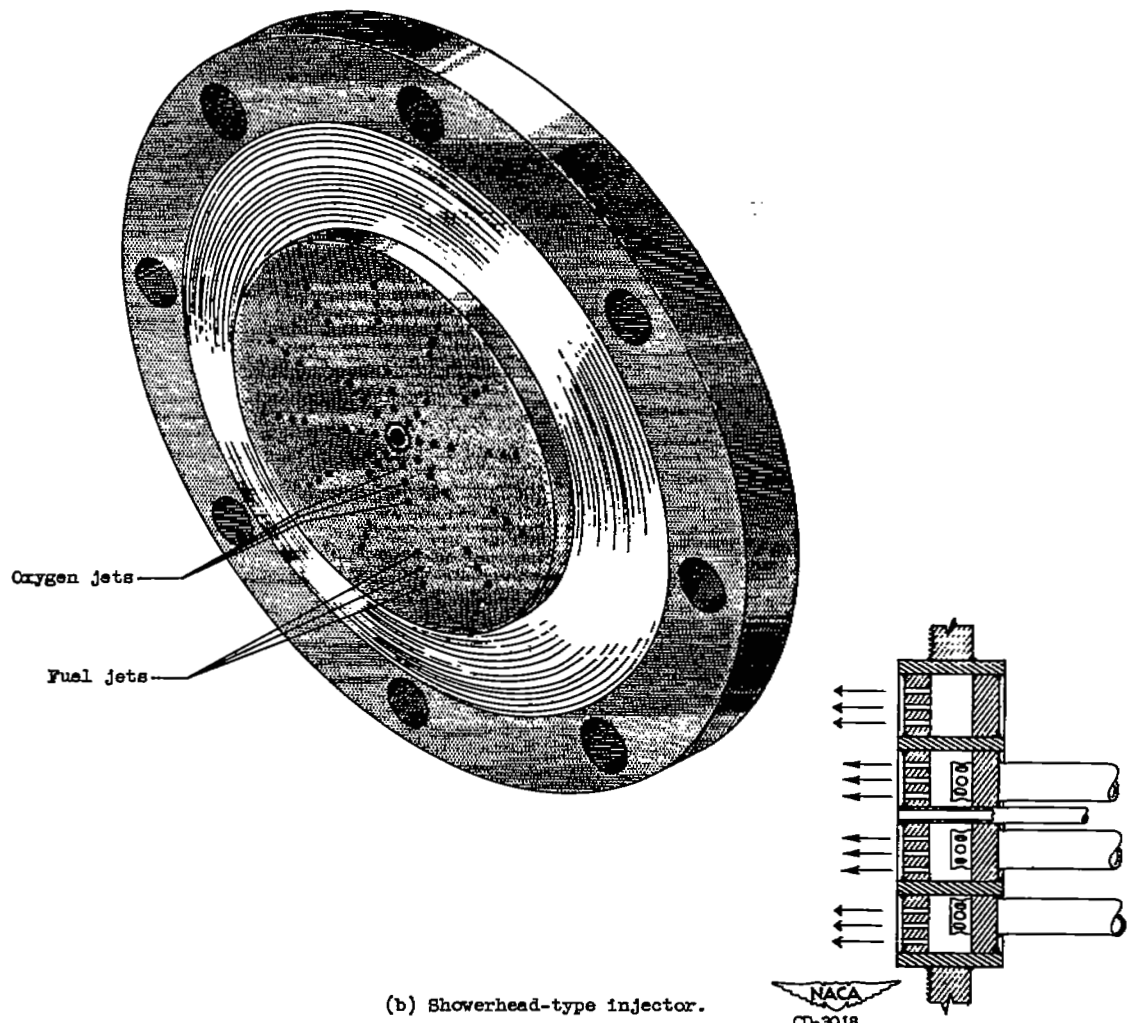


(a) Chamber and nozzle configuration.

Figure 5. - Diagrams of 500-pound thrust oxygen-fuel rocket engine.

NACA
CD-3016

2845



(b) Showerhead-type injector.

Figure 5. - Continued. Diagrams of 500-pound thrust oxygen-fuel rocket engine.

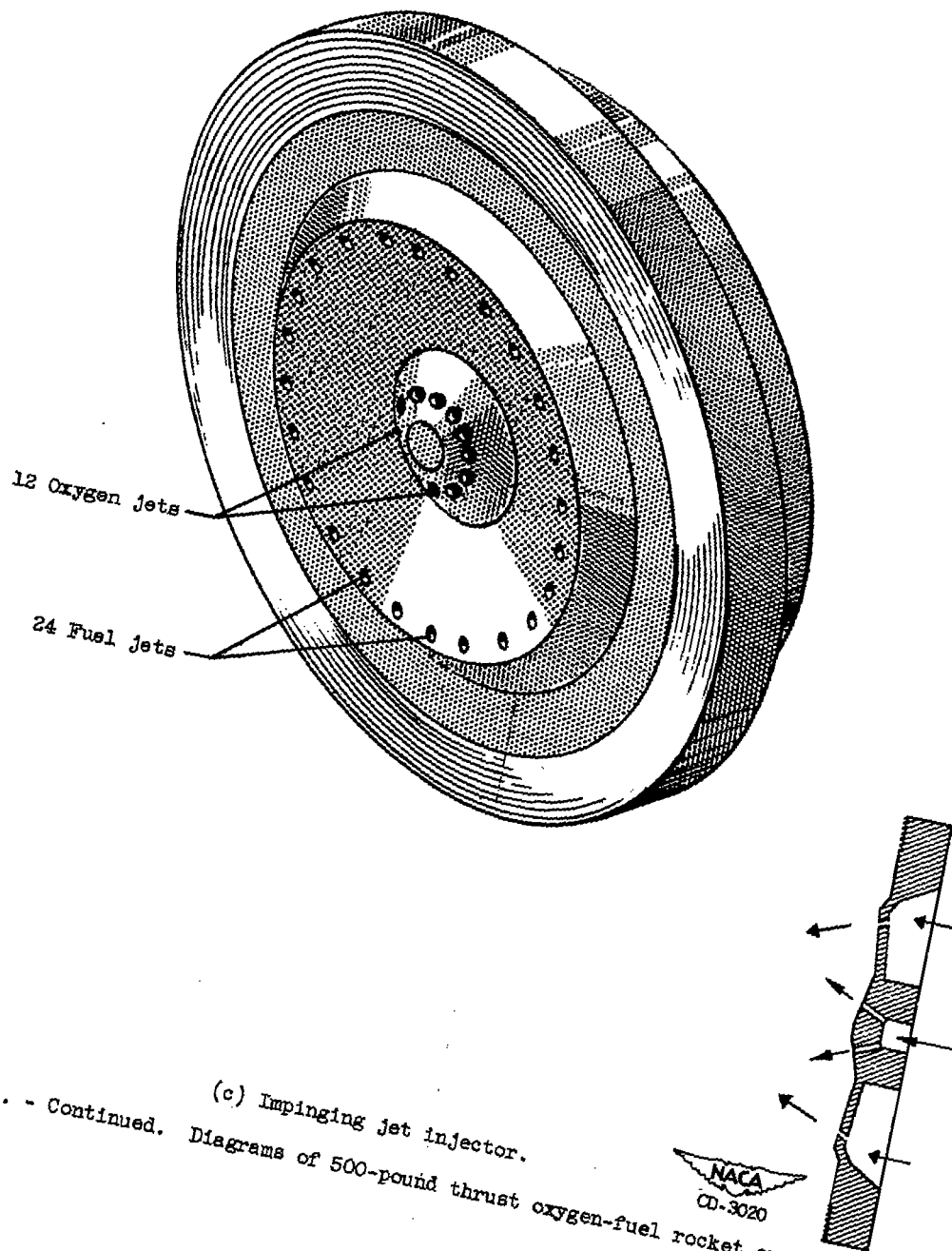
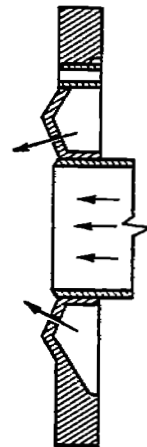
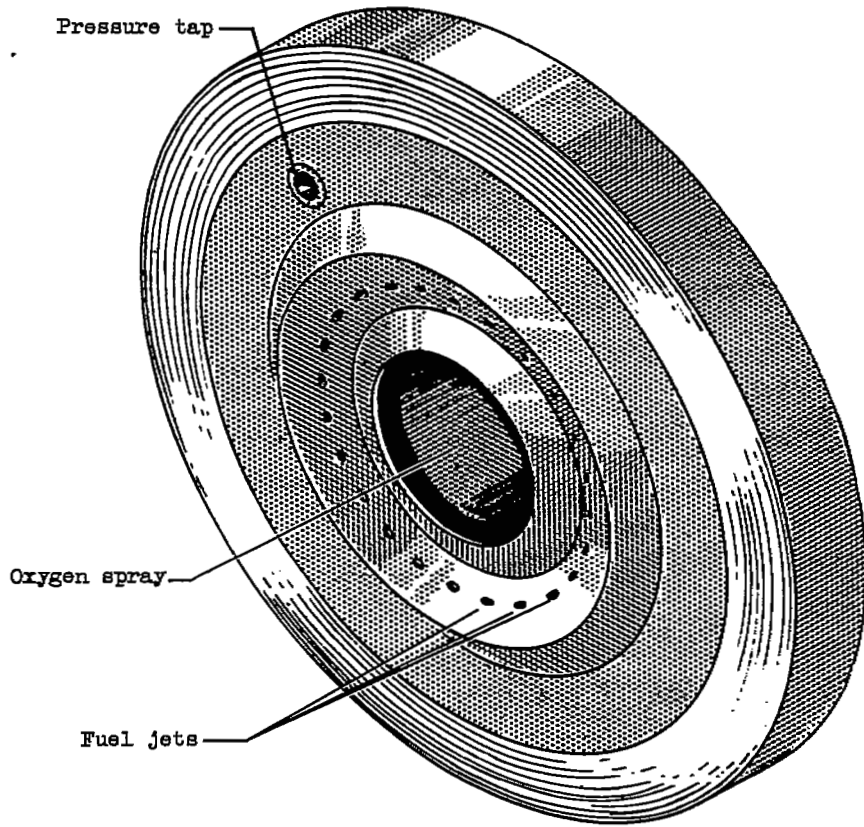


Figure 5. - Continued. Diagrams of 500-pound thrust oxygen-fuel rocket engine.

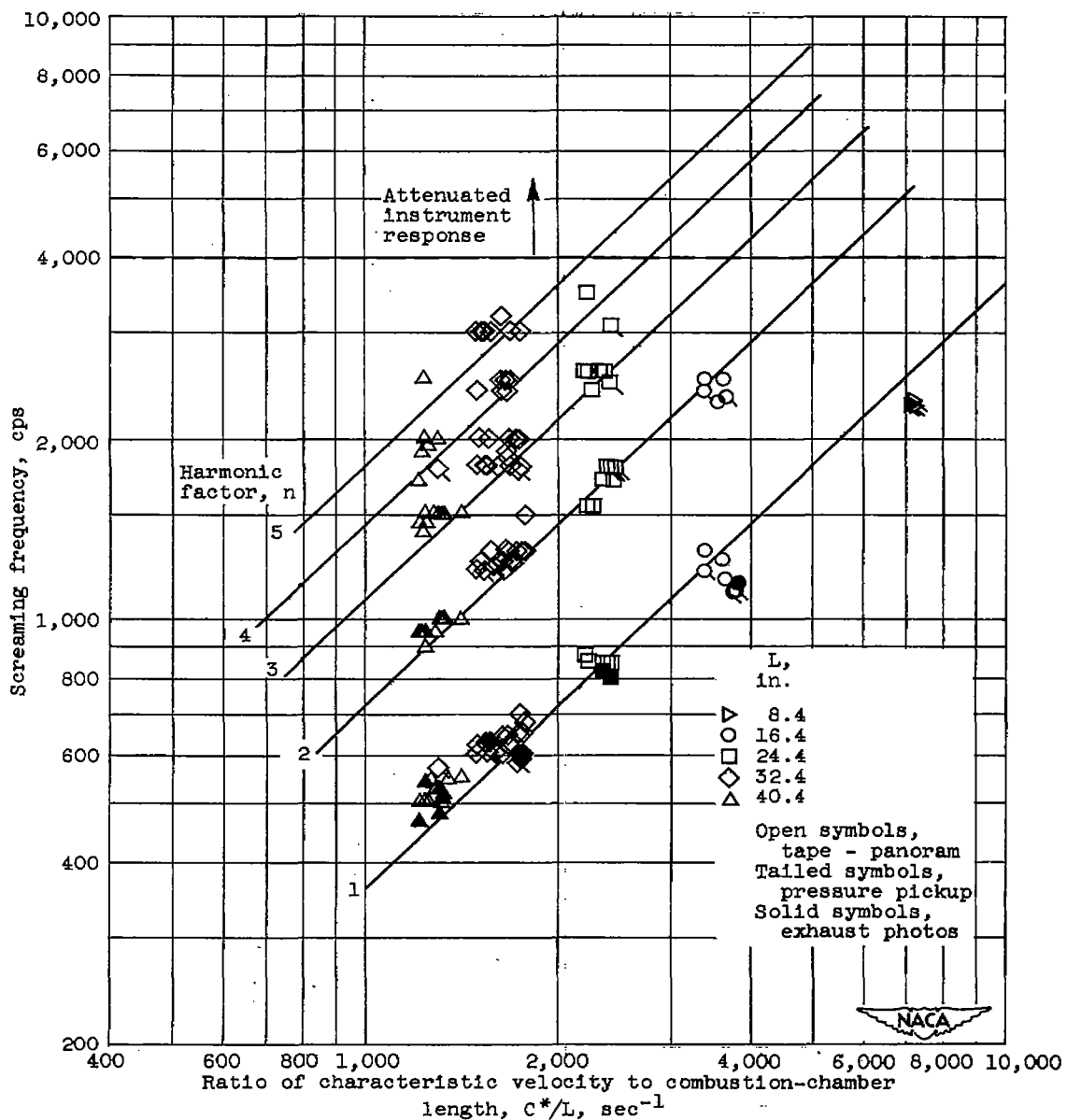
2845



NACA
CD-3019

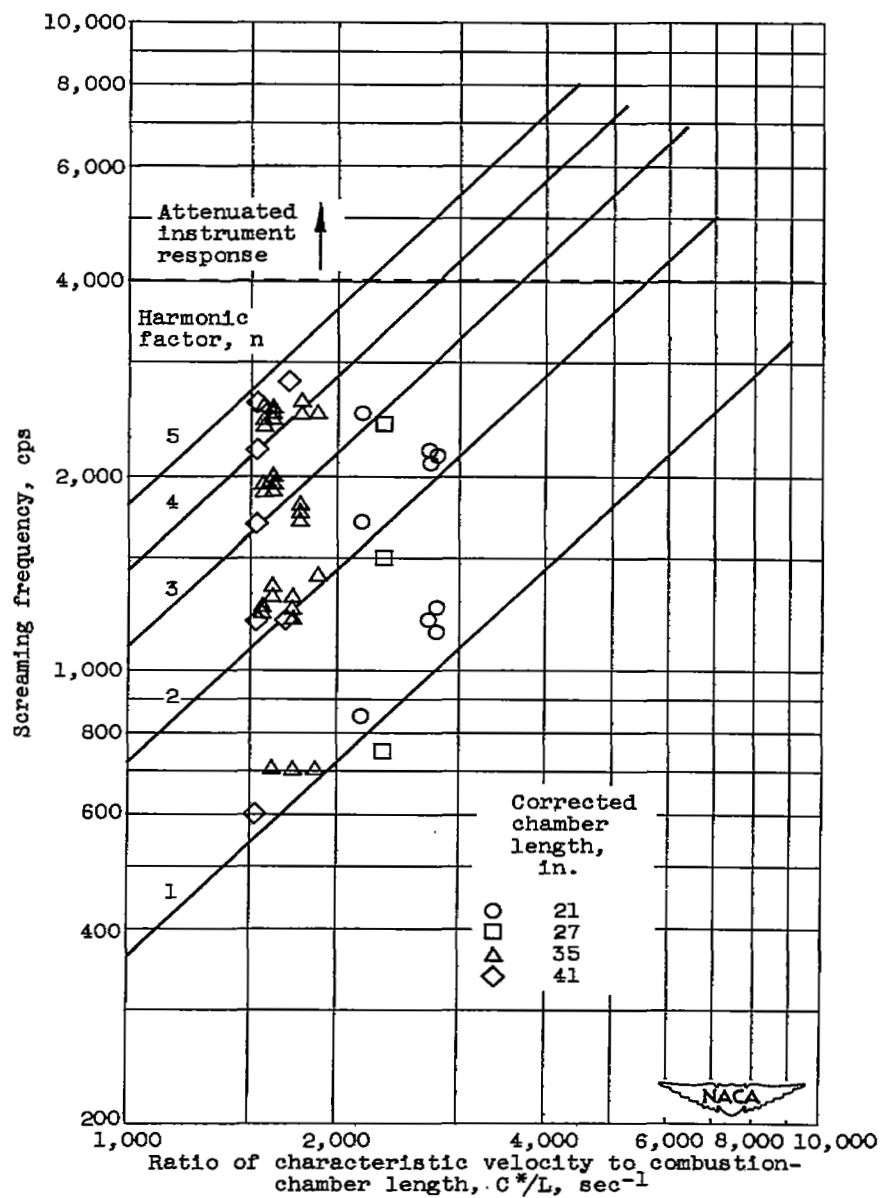
(d) Spray injector.

Figure 5. - Concluded. Diagrams of 500-pound thrust oxygen-fuel rocket engine.



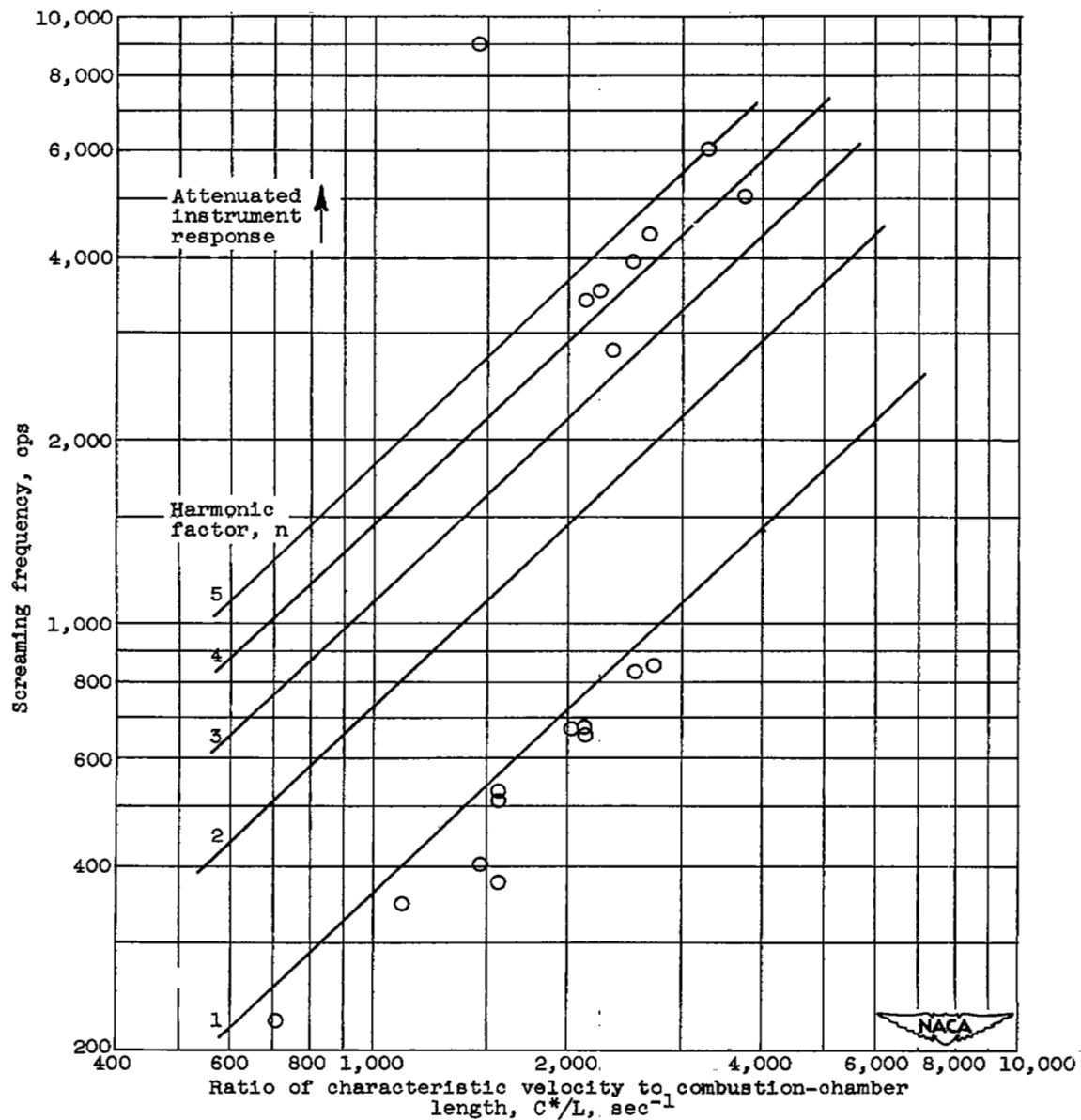
(a) Acid-hydrocarbon rocket, 100-pound thrust.

Figure 6. - Screaming frequencies plotted against ratio of characteristic velocity to combustion-chamber length. $f = 0.36 n C^*/L$.



(b) Oxygen-ammonia rocket, 500-pound thrust.

Figure 6. - Continued. Screaming frequencies plotted against ratio of characteristic velocity to combustion-chamber length. $f = 0.36 n C^*/L$.



(c) Data from other laboratories.

Figure 6. - Concluded. Screaming frequencies plotted against ratio of characteristic velocity to combustion-chamber length. $f = 0.36 n C^*/L$

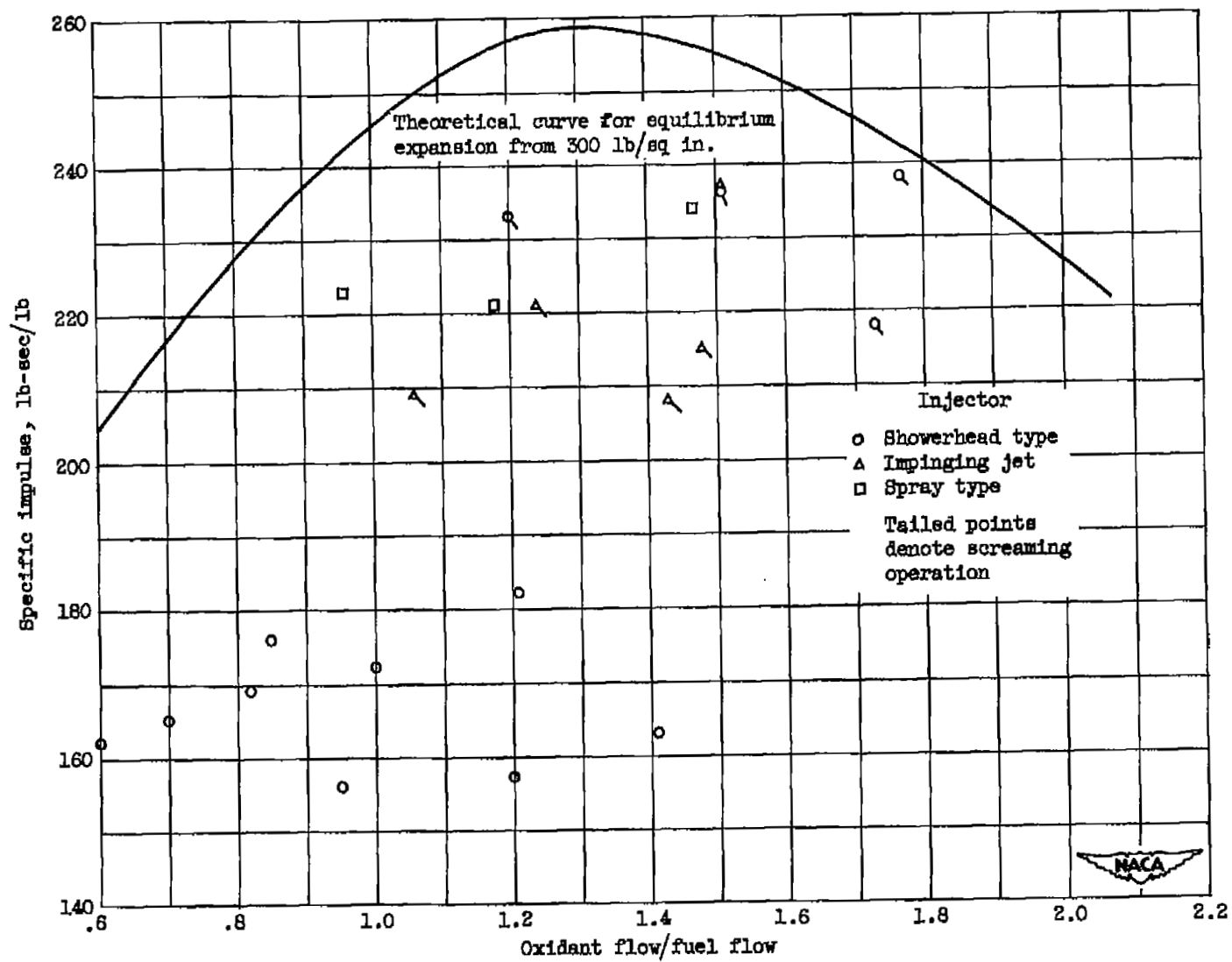


Figure 7. - Experimental performance of 500-pound-thrust oxygen-ammonia rocket engine.

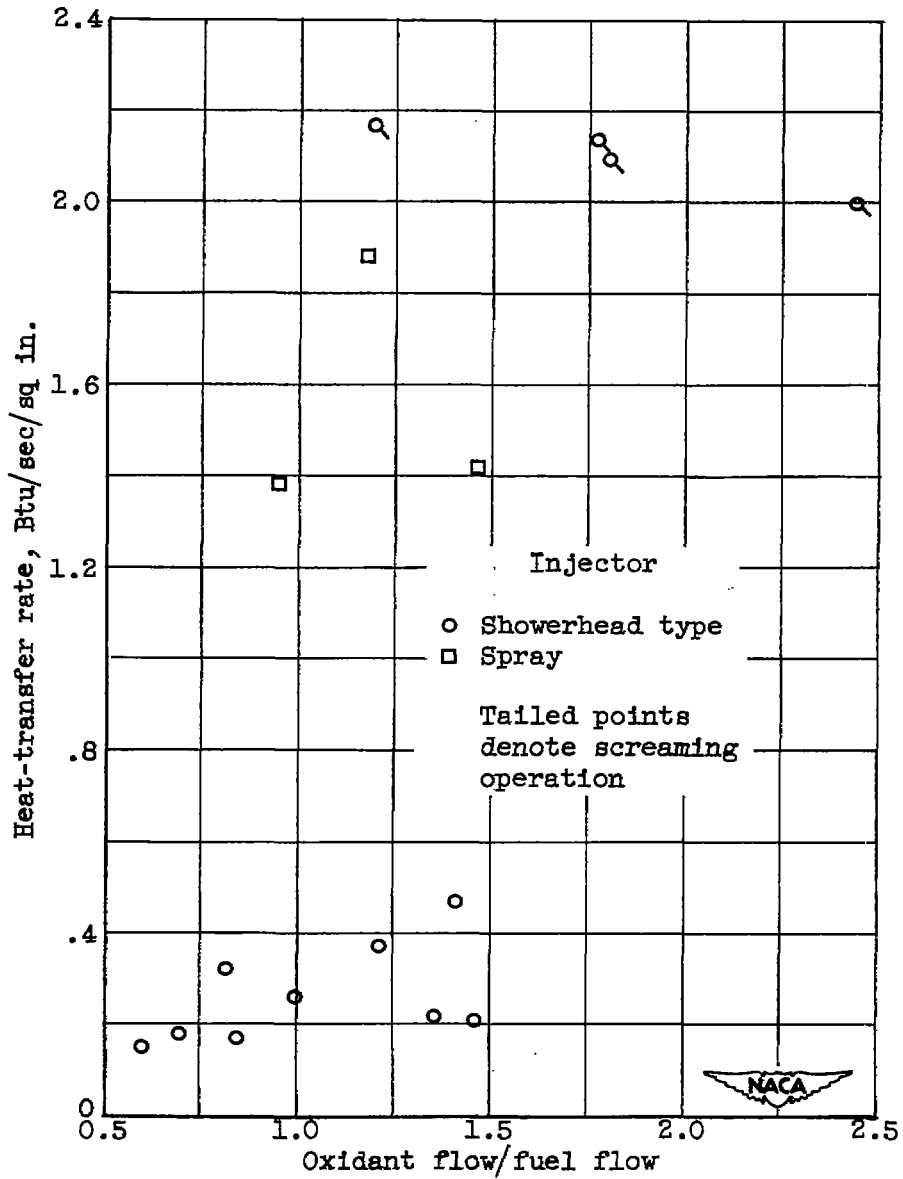


Figure 8. - Effect of screaming on heat transfer in 500-pound-thrust rocket engine with ammonia fuel.

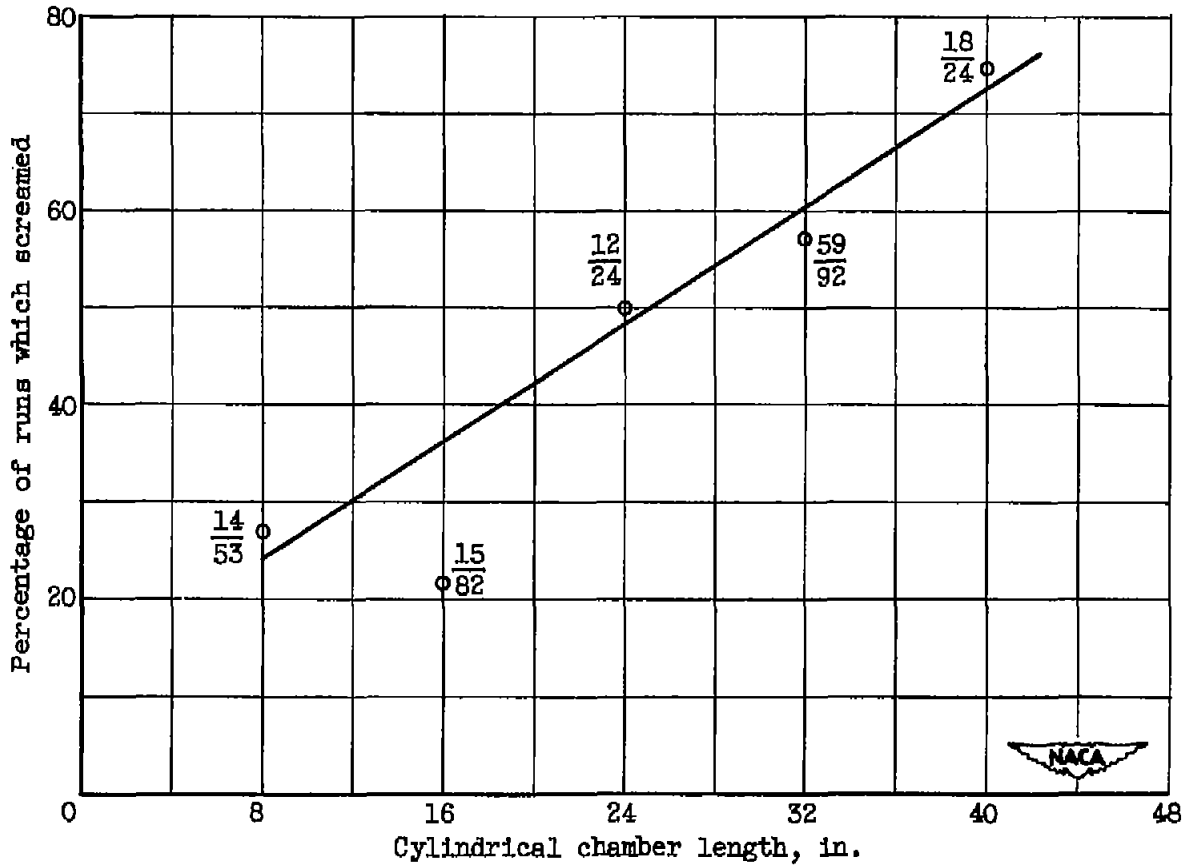


Figure 9. - Proportion of runs which screamed plotted against combustion-chamber length for acid-hydrocarbon rocket. Fractions on plot indicate number of screaming runs over total number of runs.

SECURITY INFORMATION



NASA Technical Library

3 1176 01435 6860

